Supporting Information

Polyaniline-supported Ag_2O/Mn_2O_3 nanostructures on nickel foam for efficient bifunctional water splitting electrocatalysis

Samira Akbari,[a] Zohreh Shaghaghi, [a,*] Fahimeh Farshi Azhar, [b] and Alireza Khataee [c,d]

[a] *Coordination Chemistry Research Laboratory, Department of Chemistry, Faculty of Science, Azarbaijan Shahid Madani University, Tabriz, Iran*

[b] *Department of Chemistry, Faculty of Science, Azarbaijan Shahid Madani University, Tabriz, Iran*

[c] *Department of Applied Chemistry, Faculty of Chemistry, University of Tabriz, 51666-16471, Tabriz, Iran*

[d] *Department of Chemical Engineering, Istanbul Technical University, 34469, Istanbul, Türkiye*

** Corresponding author: shaghaghi@azaruniv.ac.ir*

List of Figures and Tables

Fig. S22: FE-SEM images of the AM-1@PANI(5:1)/NF surface after the long-term stability test.

Fig. S23: Elemental mapping images of the AM-1@PANI(5:1)/NF surface after the long-term stability test.

Fig. S24: PXRD pattern of Ag_2O nanostructures hydrothermally synthesized on nickel foam.

Fig. S25: FESEM (a), and elemental mapping (b) images of Ag_2O nanostructures hydrothermally synthesized on nickel foam.

Table S1: PXRD data for all nanocompounds.

Table S2: OER important data for all prepared materials.

Table S3: HER important data for all prepared materials.

Table S4: Cell voltage value for all prepared materials in self-supported two-electrode system.

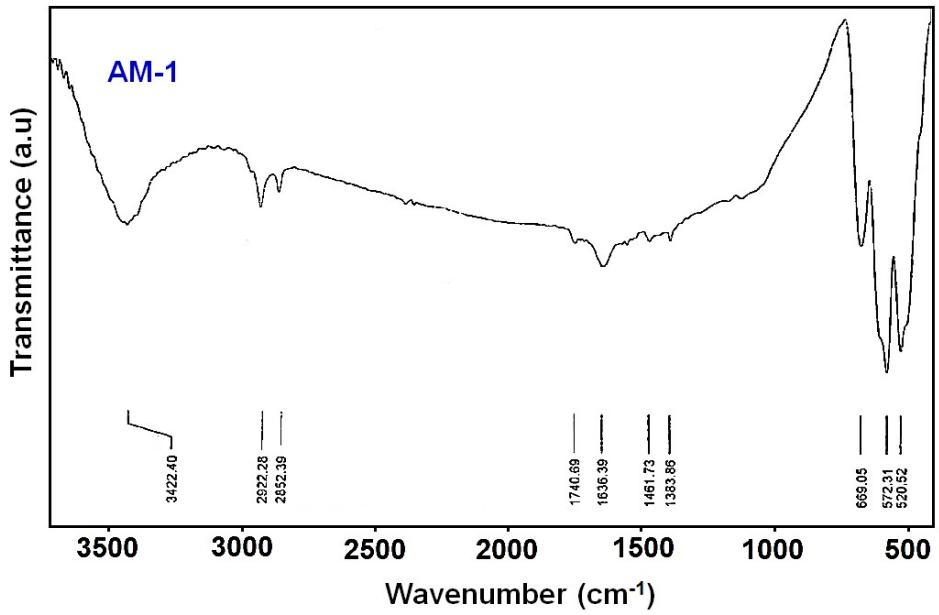

Fig. S1: FT-IR spectrum of Ag_2O/Mn_2O_3 nanostructure calcined at 550 °C (AM-1).

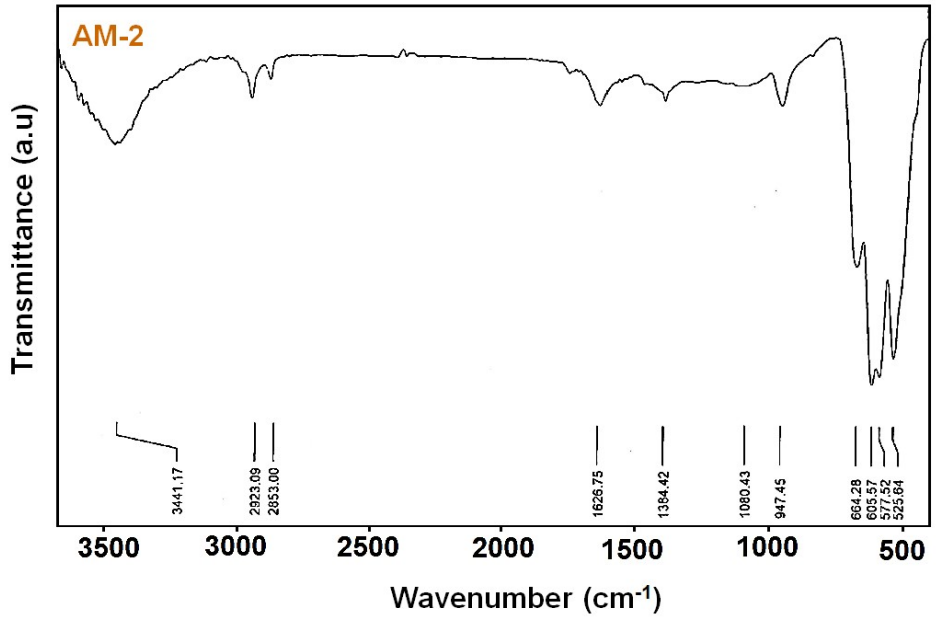

Fig. S2: FT-IR spectrum of Ag_2O/Mn_2O_3 nanostructure calcined at 650 °C (AM-2).

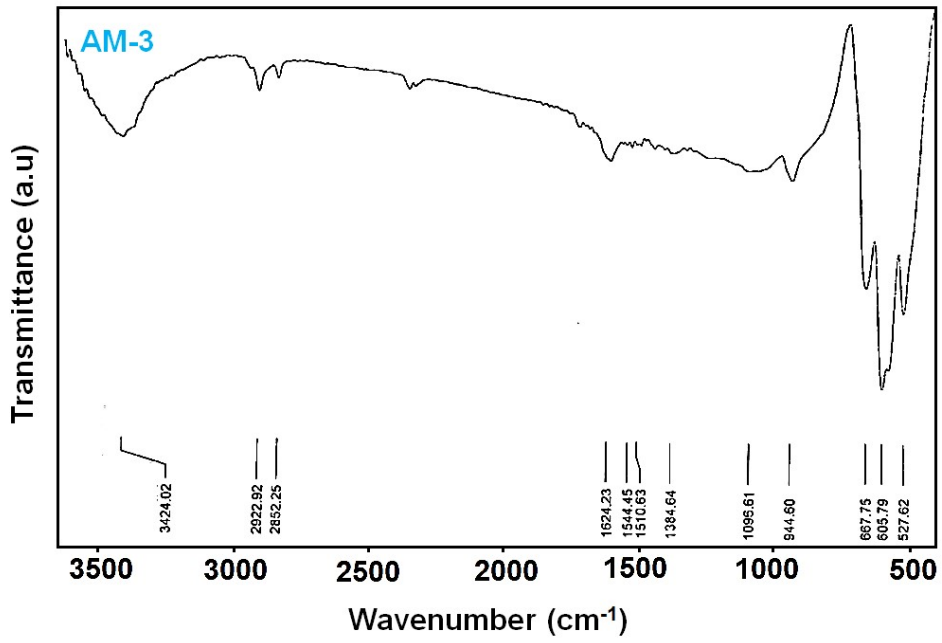

Fig. S3: FT-IR spectrum of Ag_2O/Mn_2O_3 nanostructure calcined at 700 °C (AM-3).

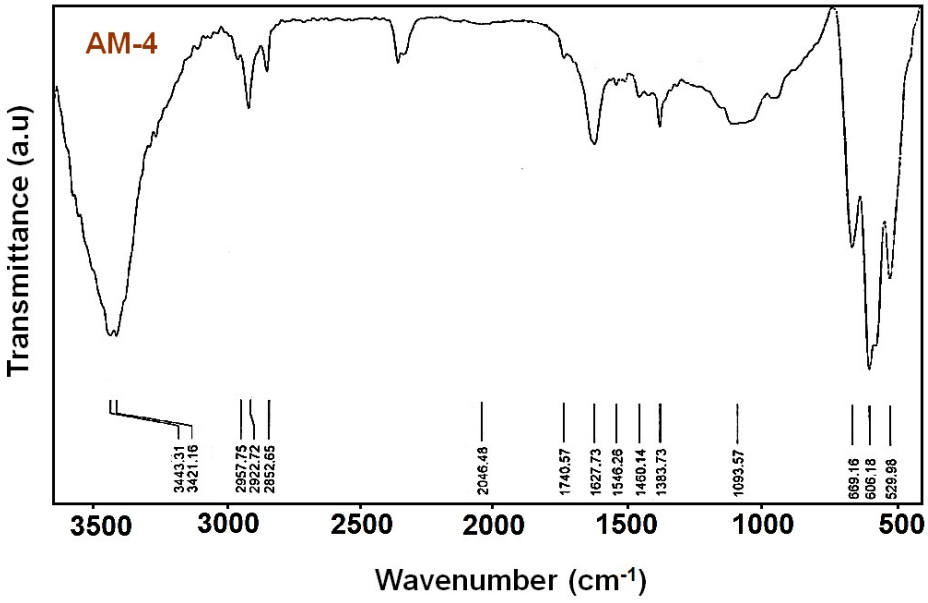

Fig. S4: FT-IR spectrum of Ag_2O/Mn_2O_3 nanostructure calcined at 750 °C (AM-4).

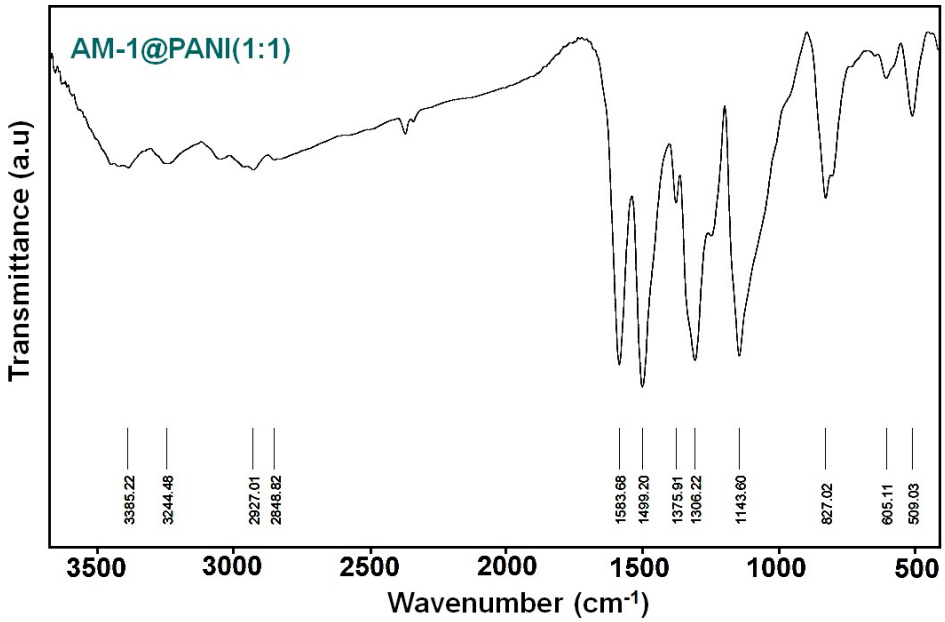

Fig. S5: FT-IR spectrum of AM-1@PANI(1:1) nanocomposite.

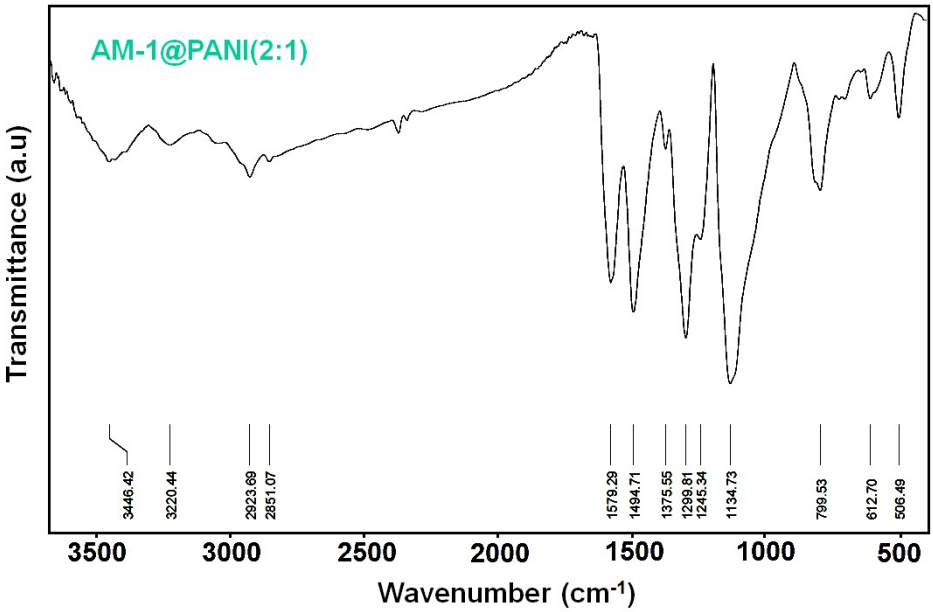

Fig. S6: FT-IR spectrum of AM-1@PANI(2:1) nanocomposite.

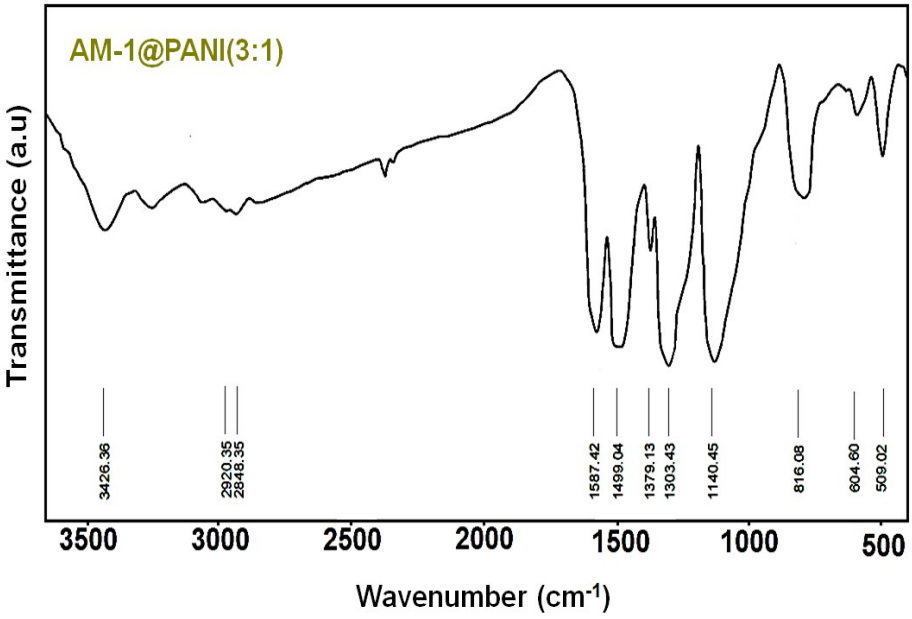

Fig. S7: FT-IR spectrum of AM-1@PANI(3:1) nanocomposite.

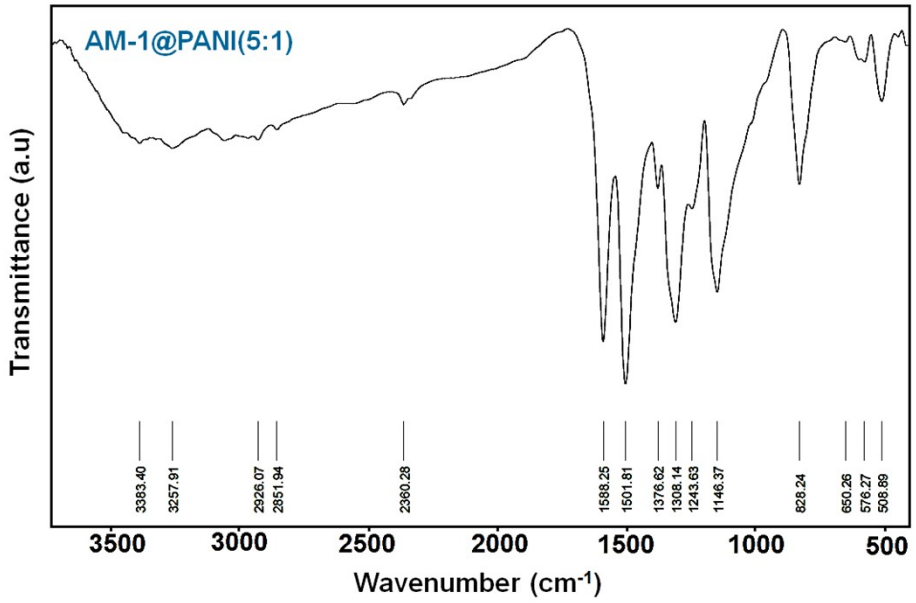

Fig. S8: FT-IR spectrum of AM-1@PANI(5:1) nanocomposite.

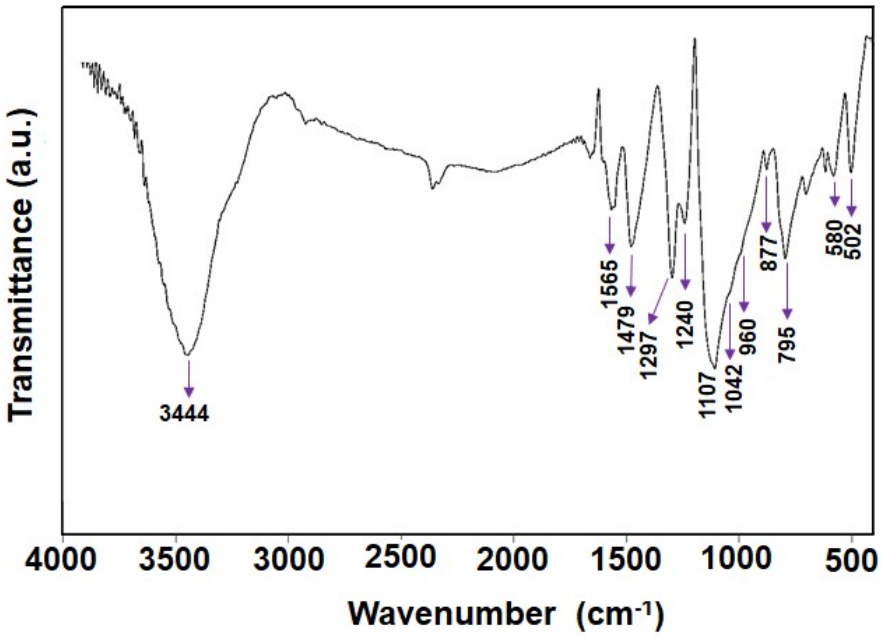

Fig. S9: FT-IR spectrum of PANI.

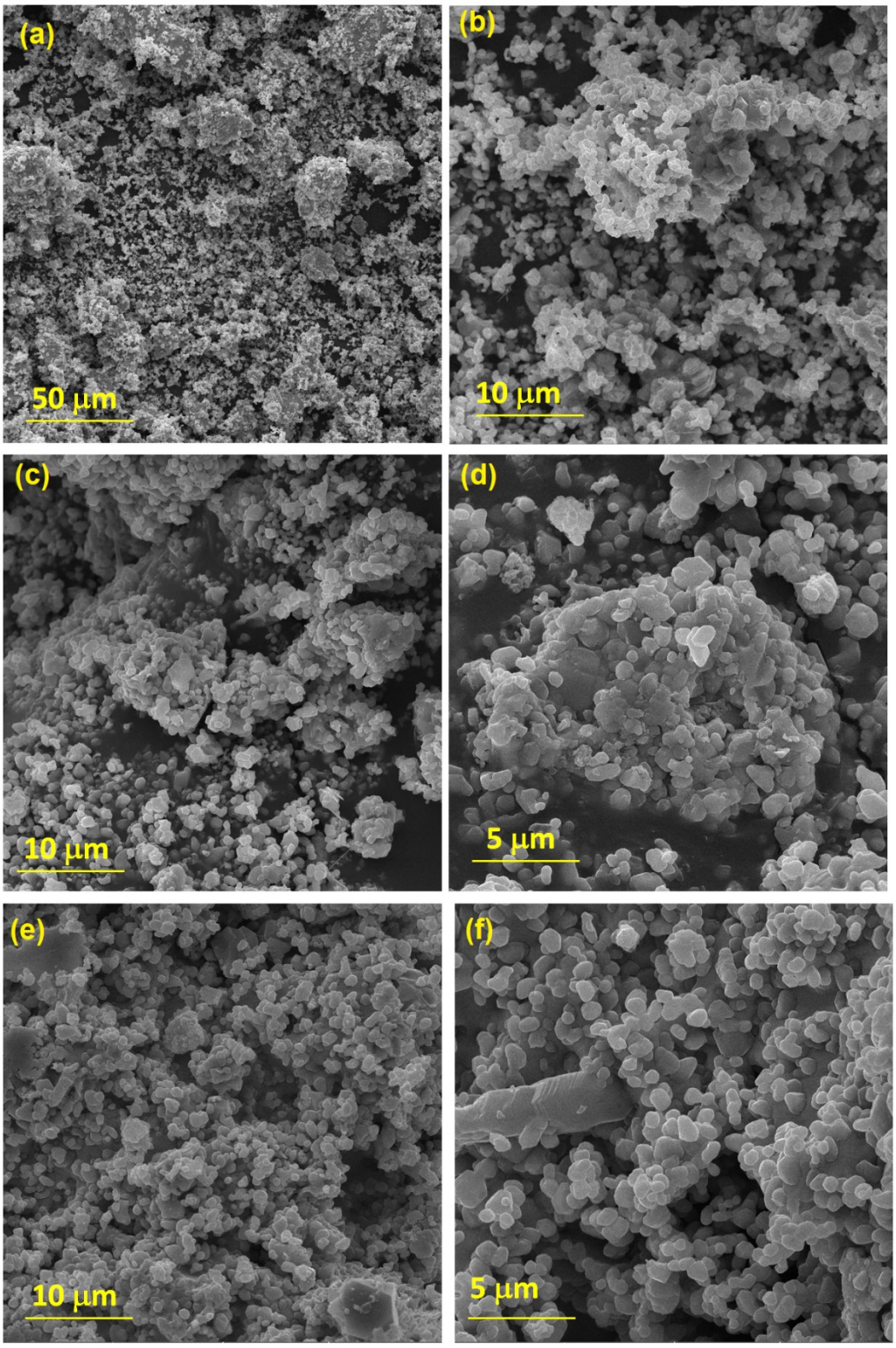

Fig. S10: FESEM images of AM-2 (calcined at 650 °C) (a and b), AM-3 (calcined at 700 °C) (c and d), and AM-4 (calcined at 750 °C) (e and f).

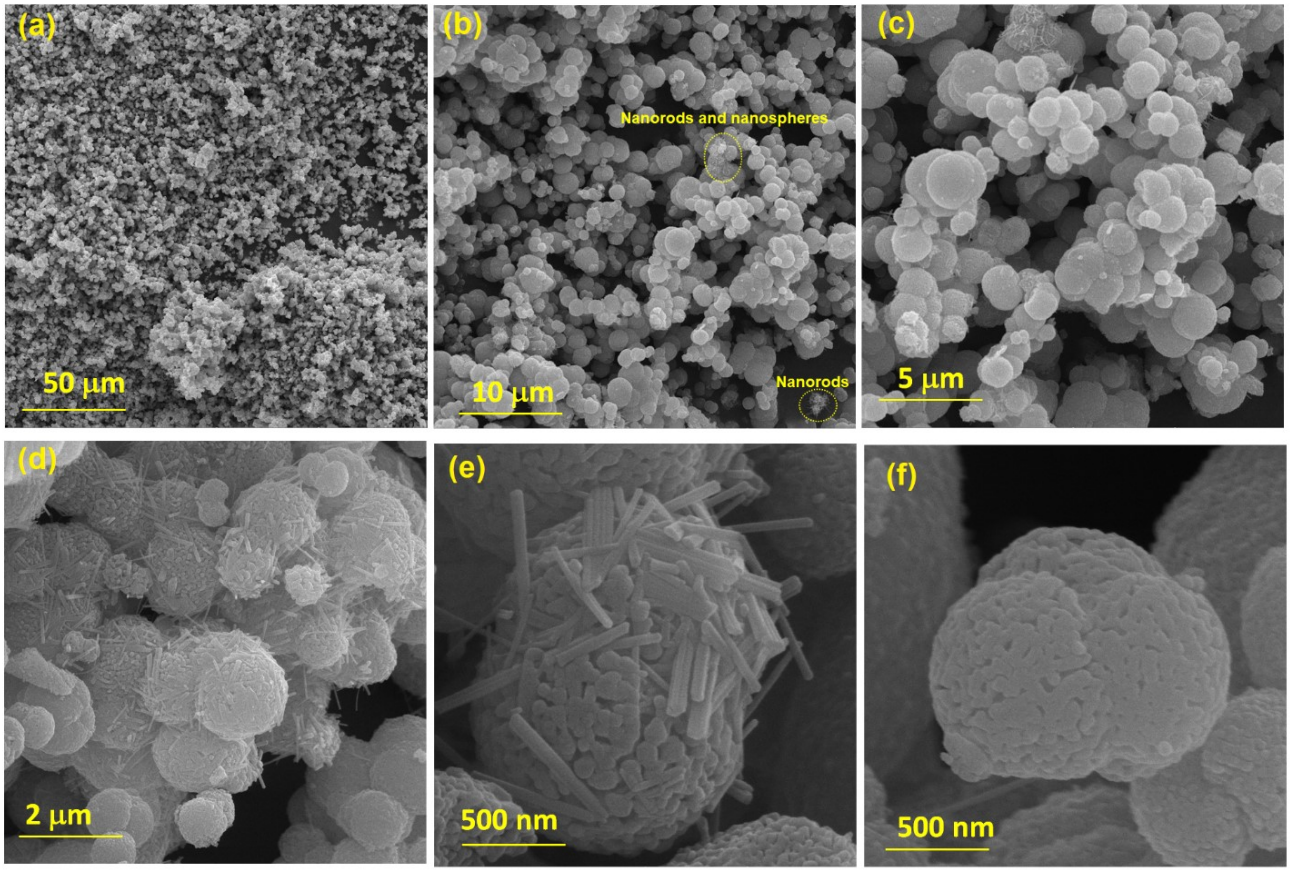

Fig. S11: FESEM images of Mn_2O_3 nanostructure.

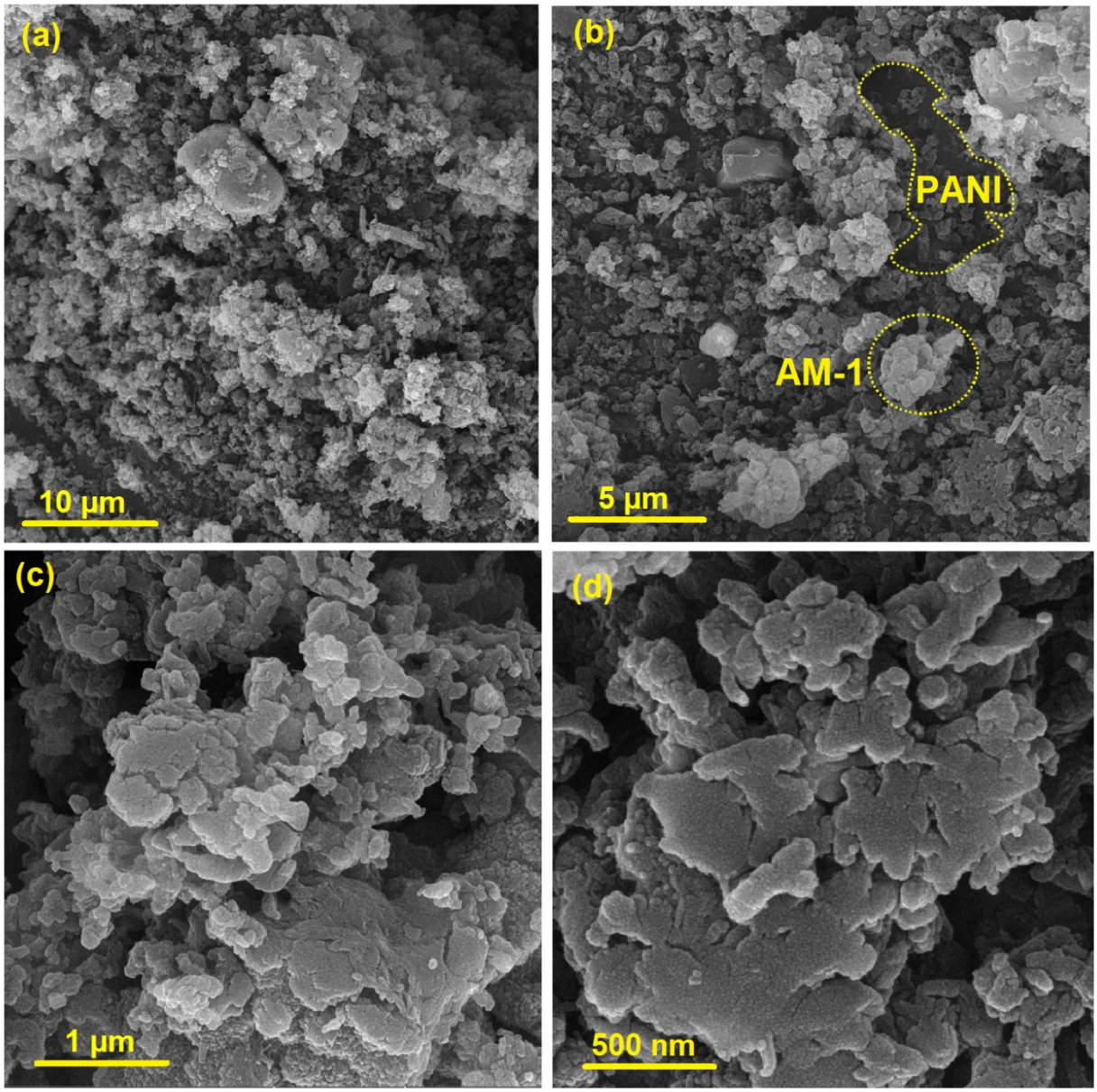

Fig. S12: FESEM images of AM-1@PANI(1:1) nanocomposite.

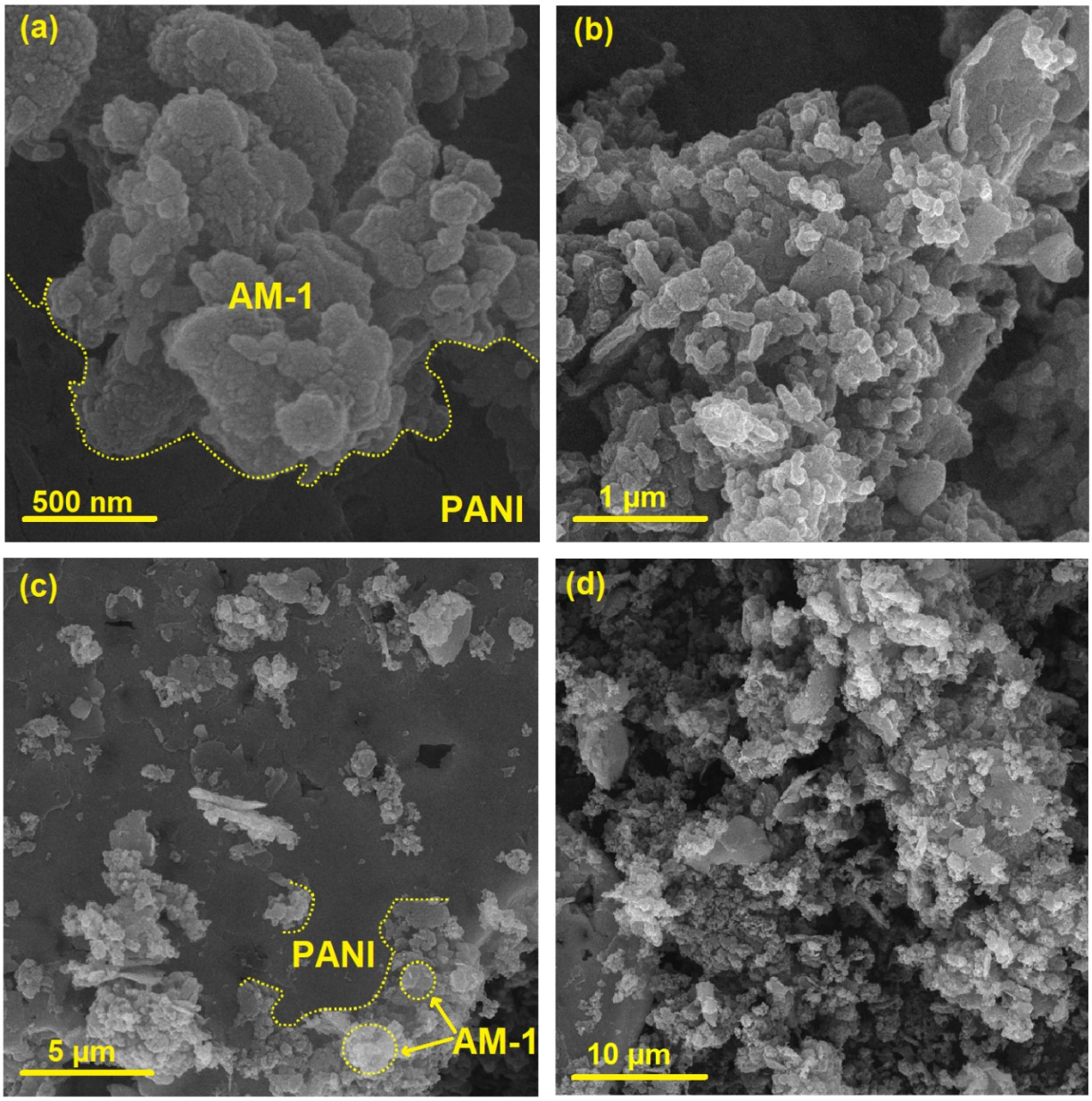

Fig. S13: FESEM images of AM-1@PANI(2:1) nanocomposite.

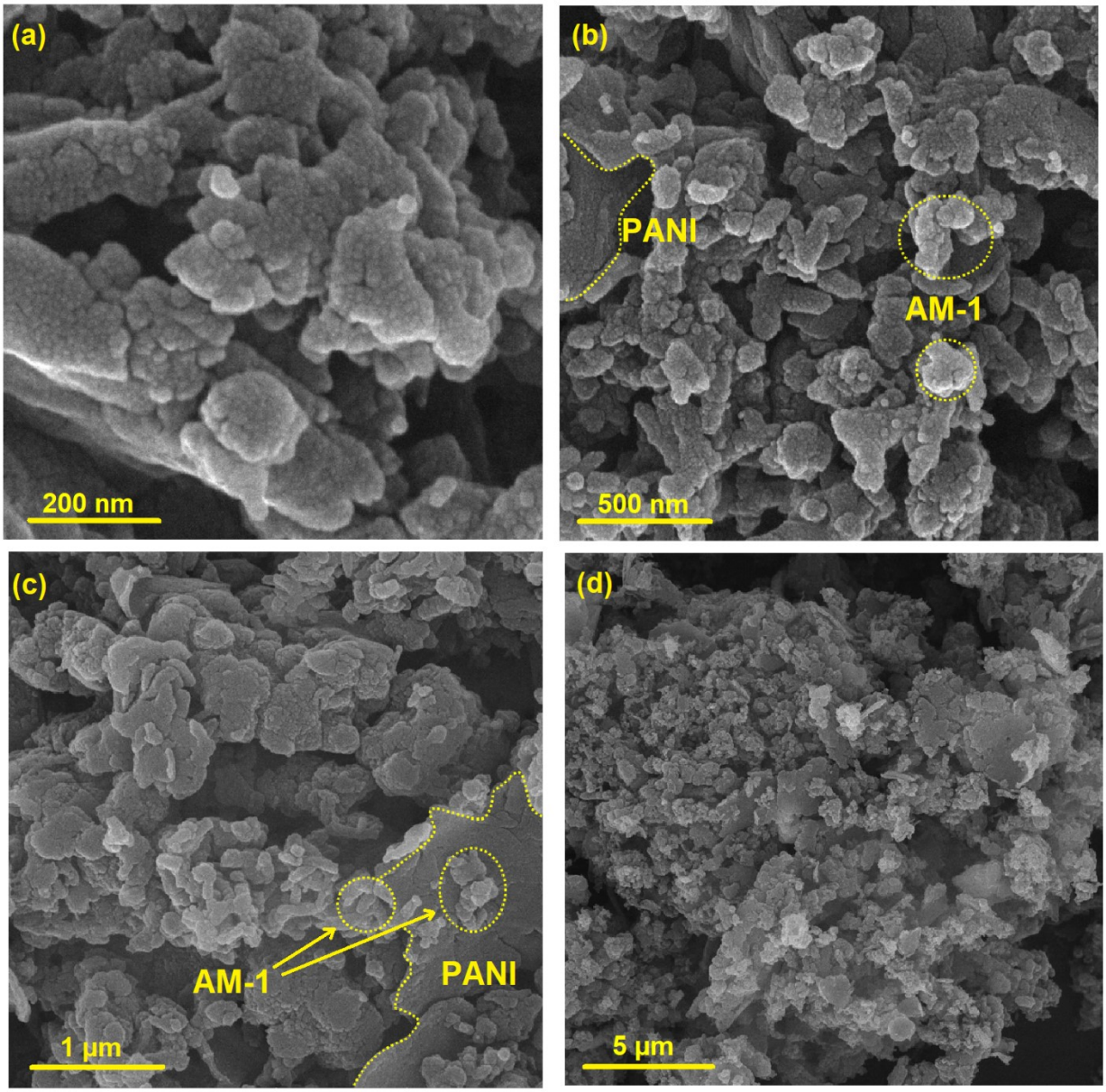

Fig. S14: FESEM images of AM-1@PANI(3:1) nanocomposite.

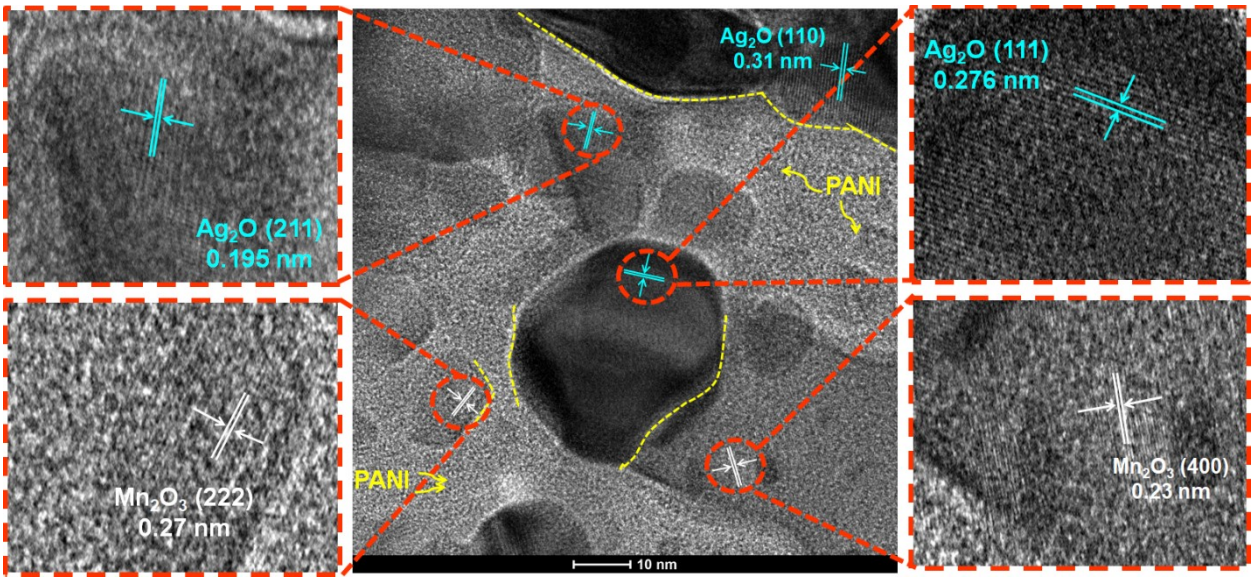

Fig. S15: High-resolution TEM image for AM-1@PANI(5:1) nanocomposite.

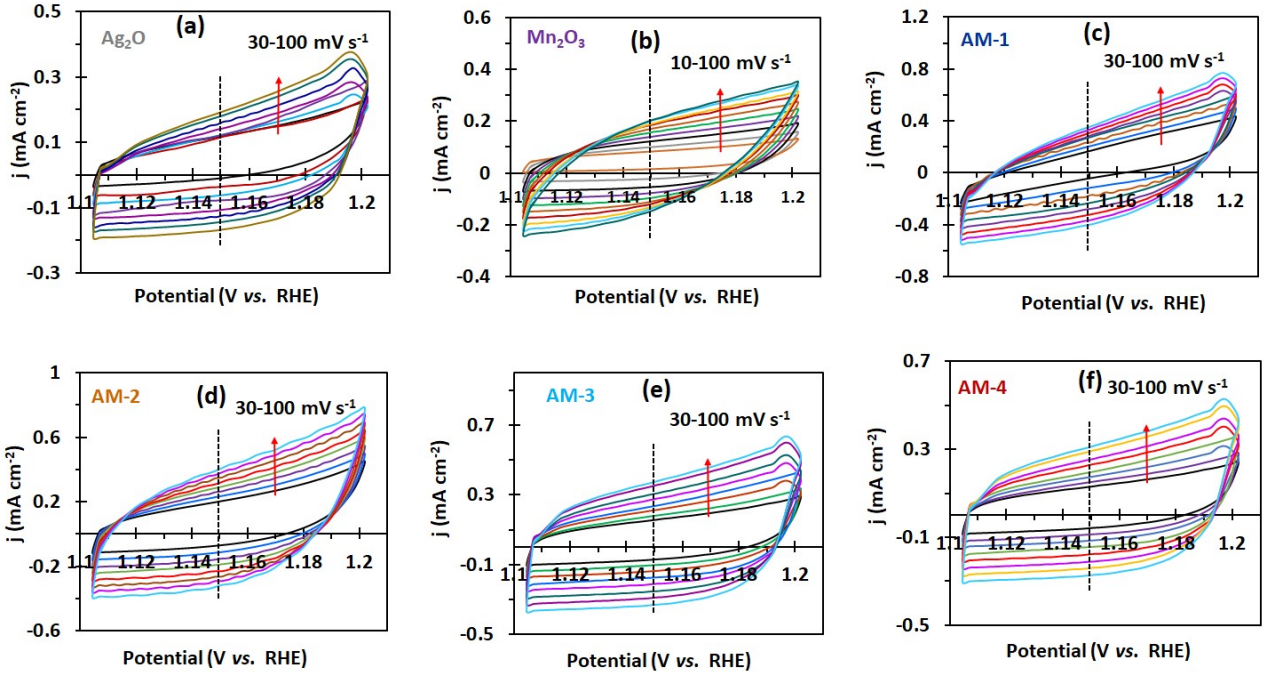

Fig. S16: CVs at different scan rates of 30-100 mV s^{-1} in the non-faradaic range of 1.1-1.2 V *vs.* RHE for pure Ag_2O, pure Mn_2O_3, and Ag_2O/Mn_2O_3 nanostructures calcined at different temperatures.

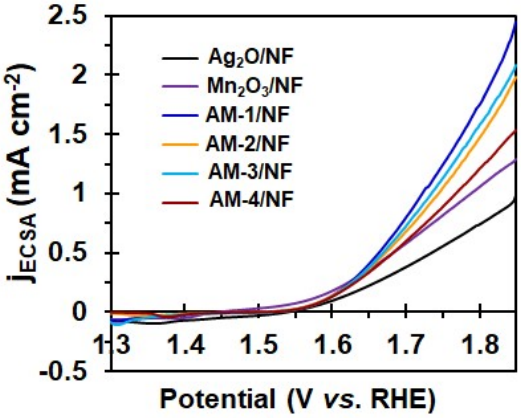

Fig. S17: Normalized LSV curves for Ag_2O, Mn_2O_3, and Ag_2O/Mn_2O_3 (AM) nanostructures, indicating their activity in OER for the ECSA calculation, the C_s value was assumed to be 40 μF cm^{-2}, and the C_{dl} value for Mn_2O_3 was obtained from CVs recorded in different scan rates of 10-60 mV s^{-1}).

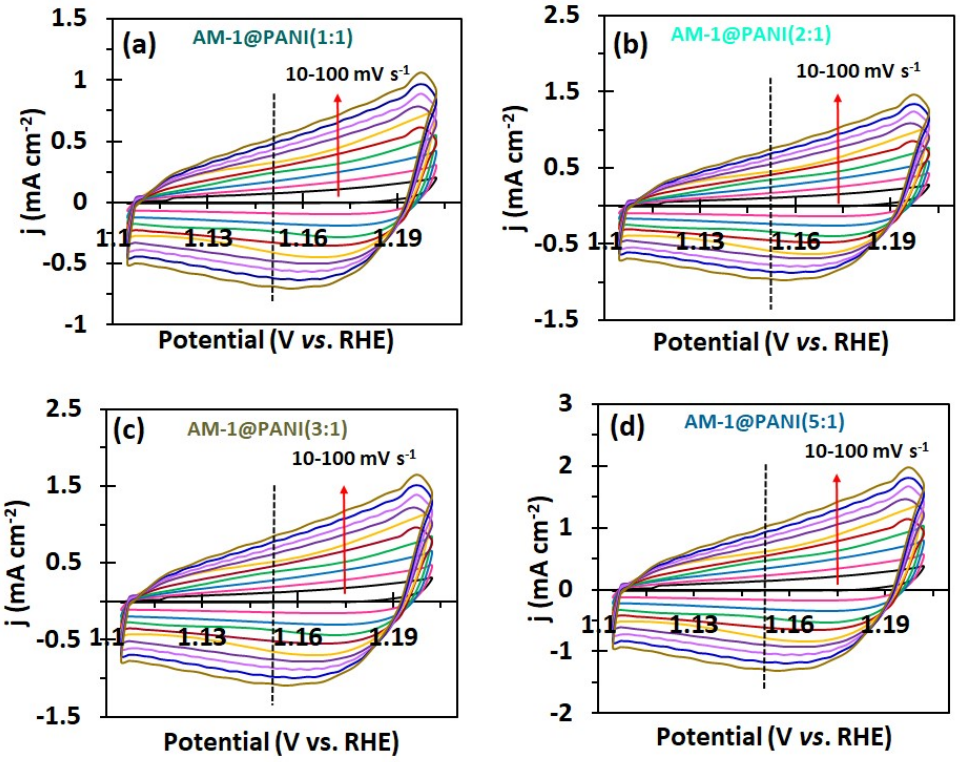

Fig. S18: CVs at different scan rates of 30-100 mV s^{-1} in the non-faradaic range of 1.1-1.2 V *vs.* RHE for pure AM-1@PANI nanocomposites with the weight ratios of 1:1, 2:1, 3:1, and 5:1 from AM-1 to PANI.

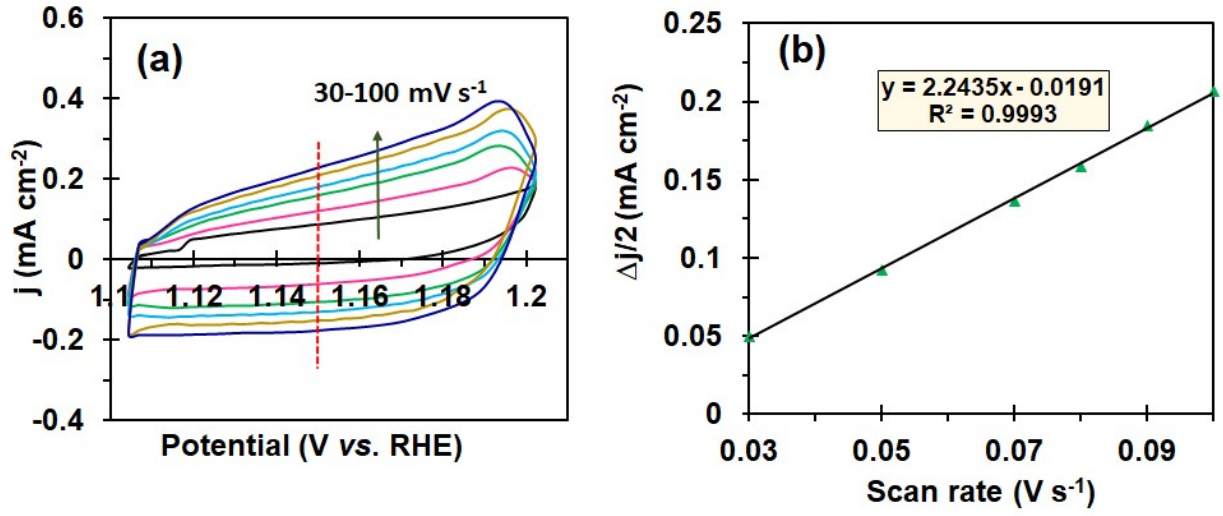

Fig. S19: CVs at different scan rates of 30-100 mV s^{-1} in the non-faradaic range of 1.1-1.2 V *vs*. RHE for pure PANI (a), and the corresponding C_{dl} (b).

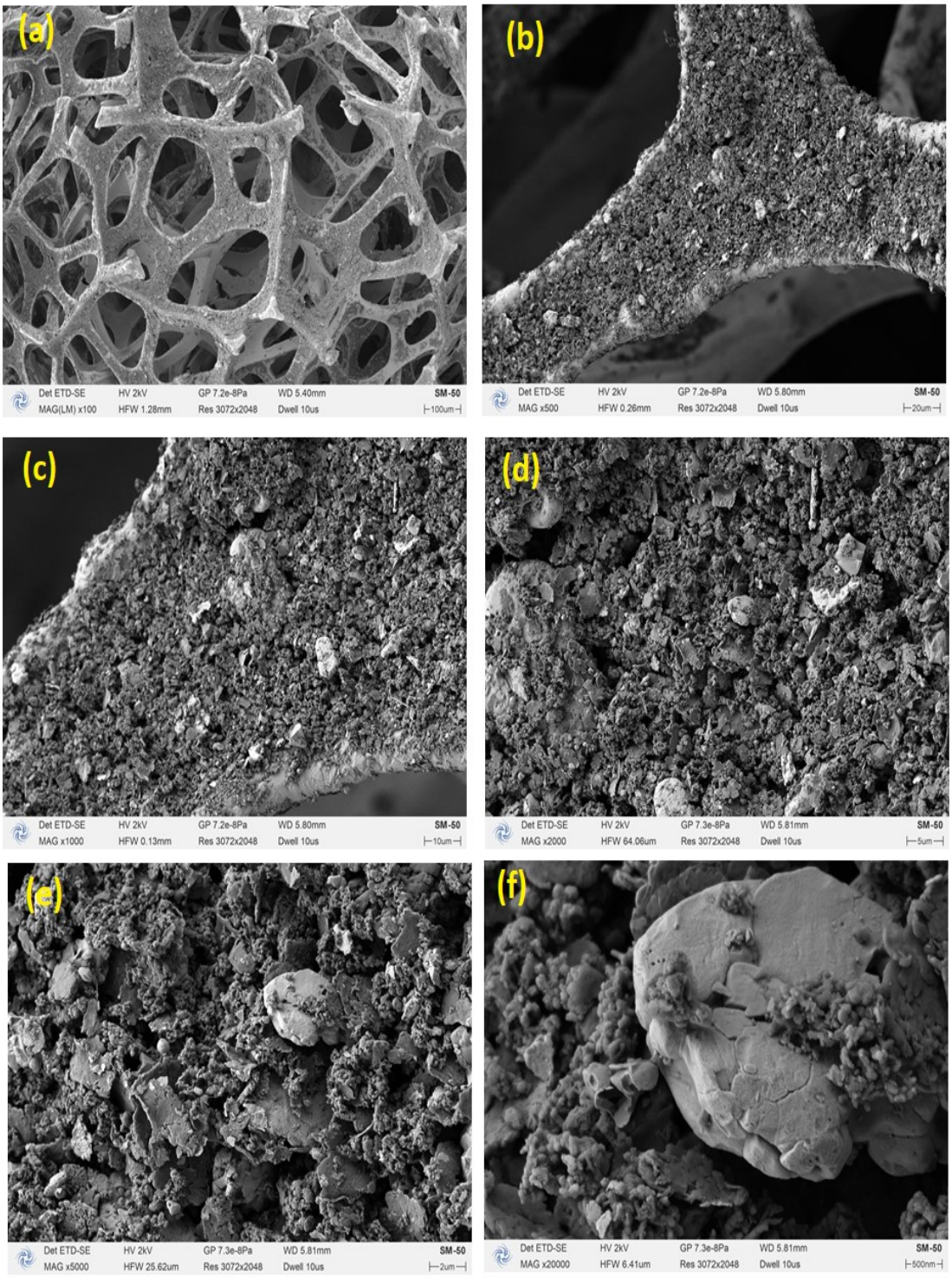

Fig. S20: FE-SEM images of surface of the AM-1@PANI(5:1)/NF surface before the long-term stability test.

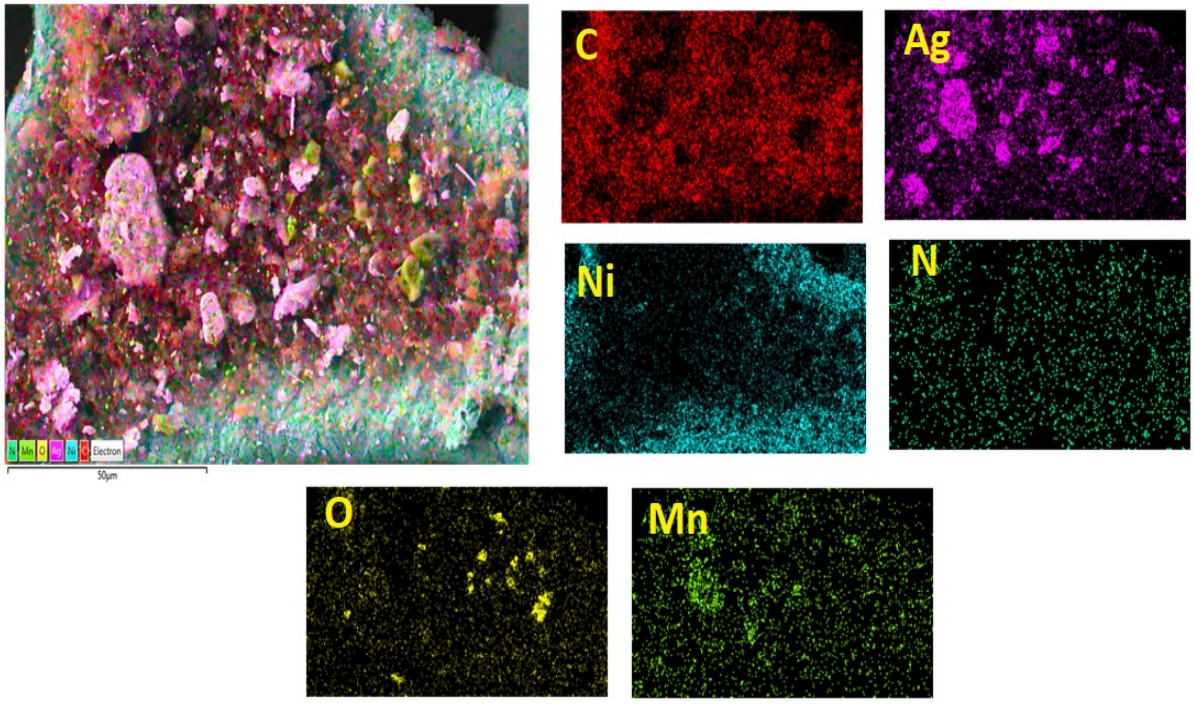

Fig. S21: Elemental mapping images of the AM-1@PANI(5:1)/NF surface before the long-term stability test.

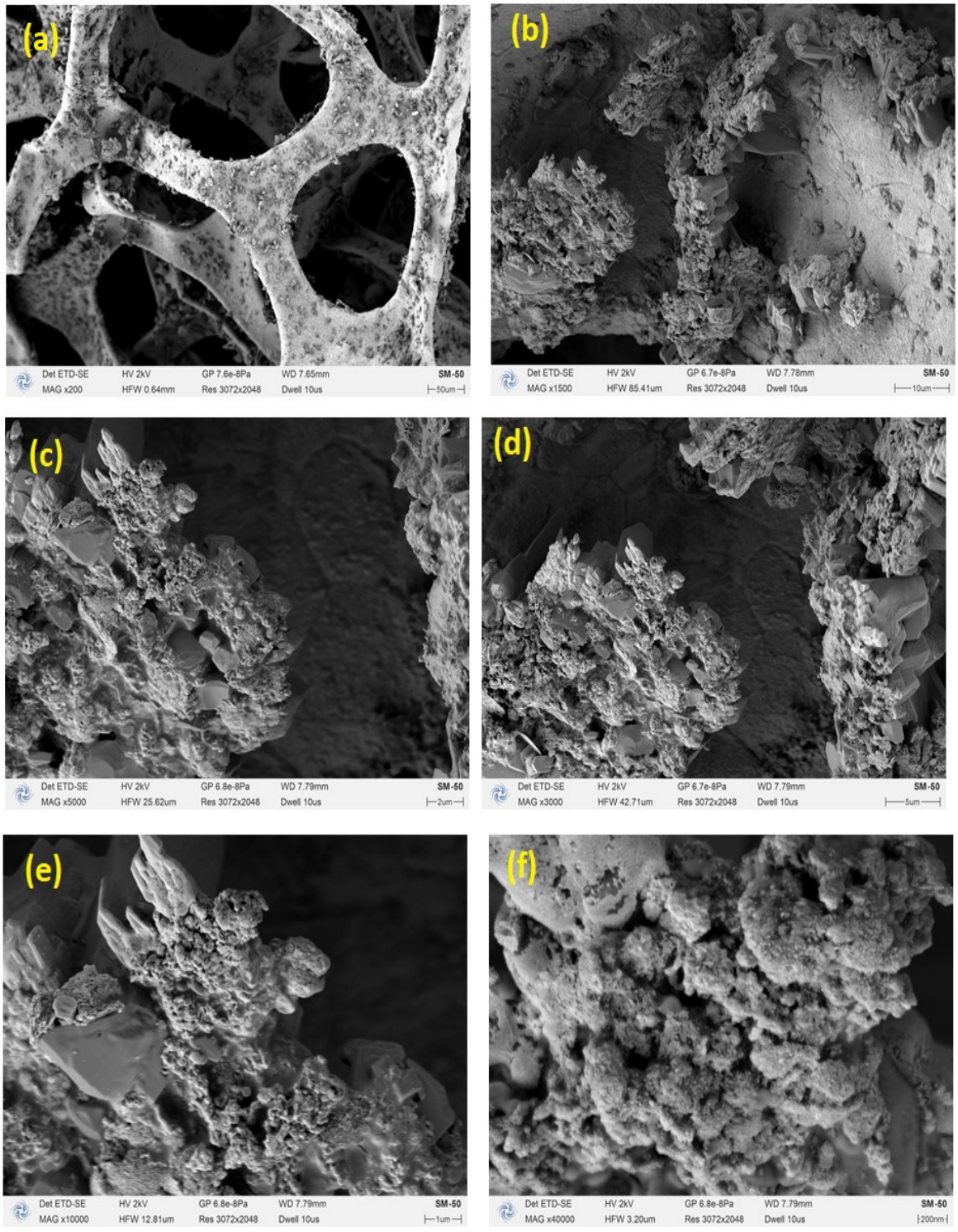

Fig. S22: FE-SEM images of the AM-1@PANI(5:1)/NF surface after the long-term stability test.

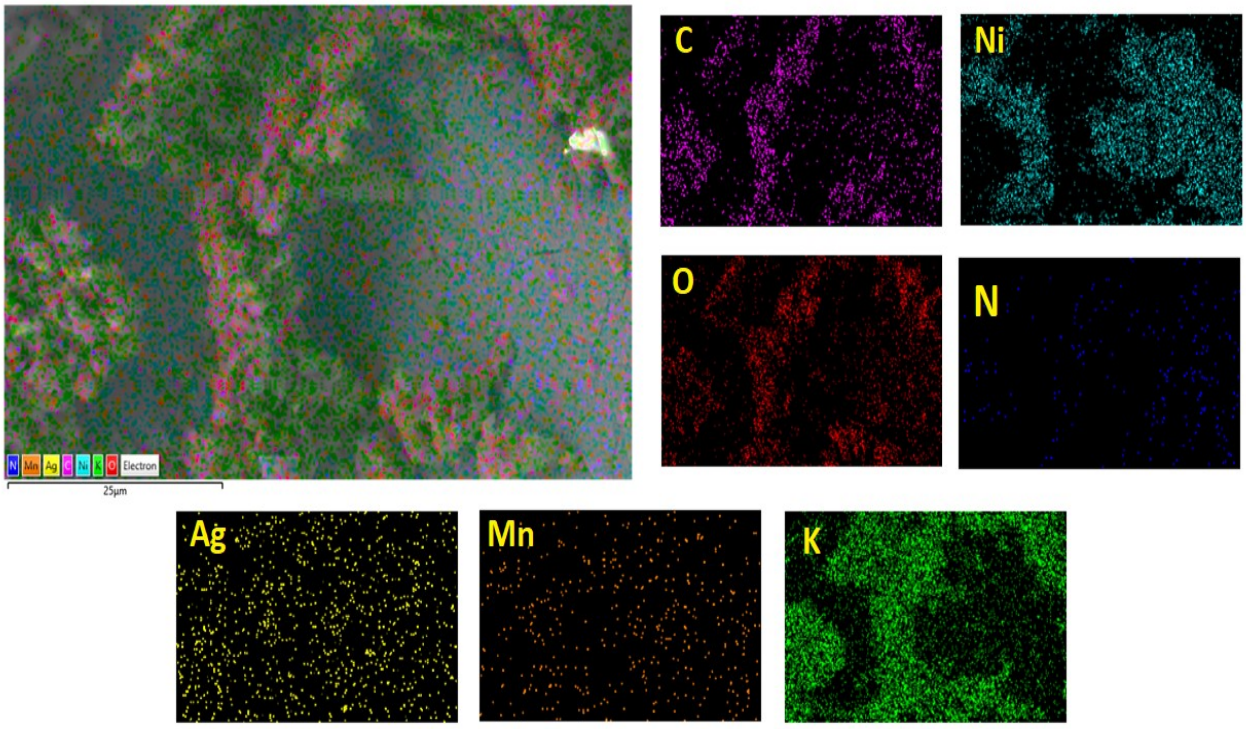

Fig. S23: Elemental mapping images of the AM-1@PANI(5:1)/NF surface after the long-term stability test.

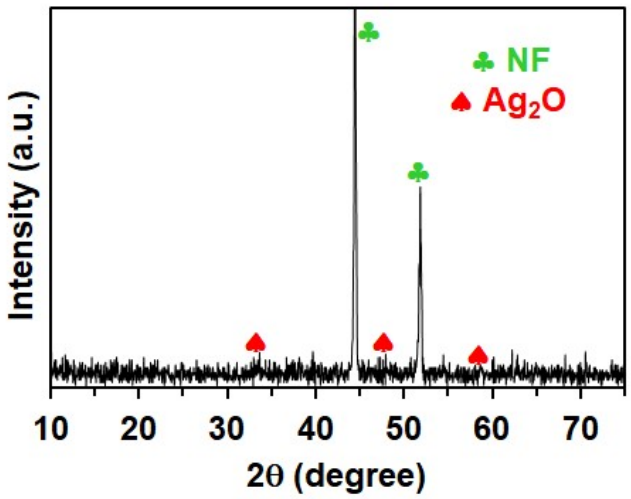

Fig. S24: PXRD pattern of Ag_2O nanostructures hydrothermally synthesized on nickel foam.

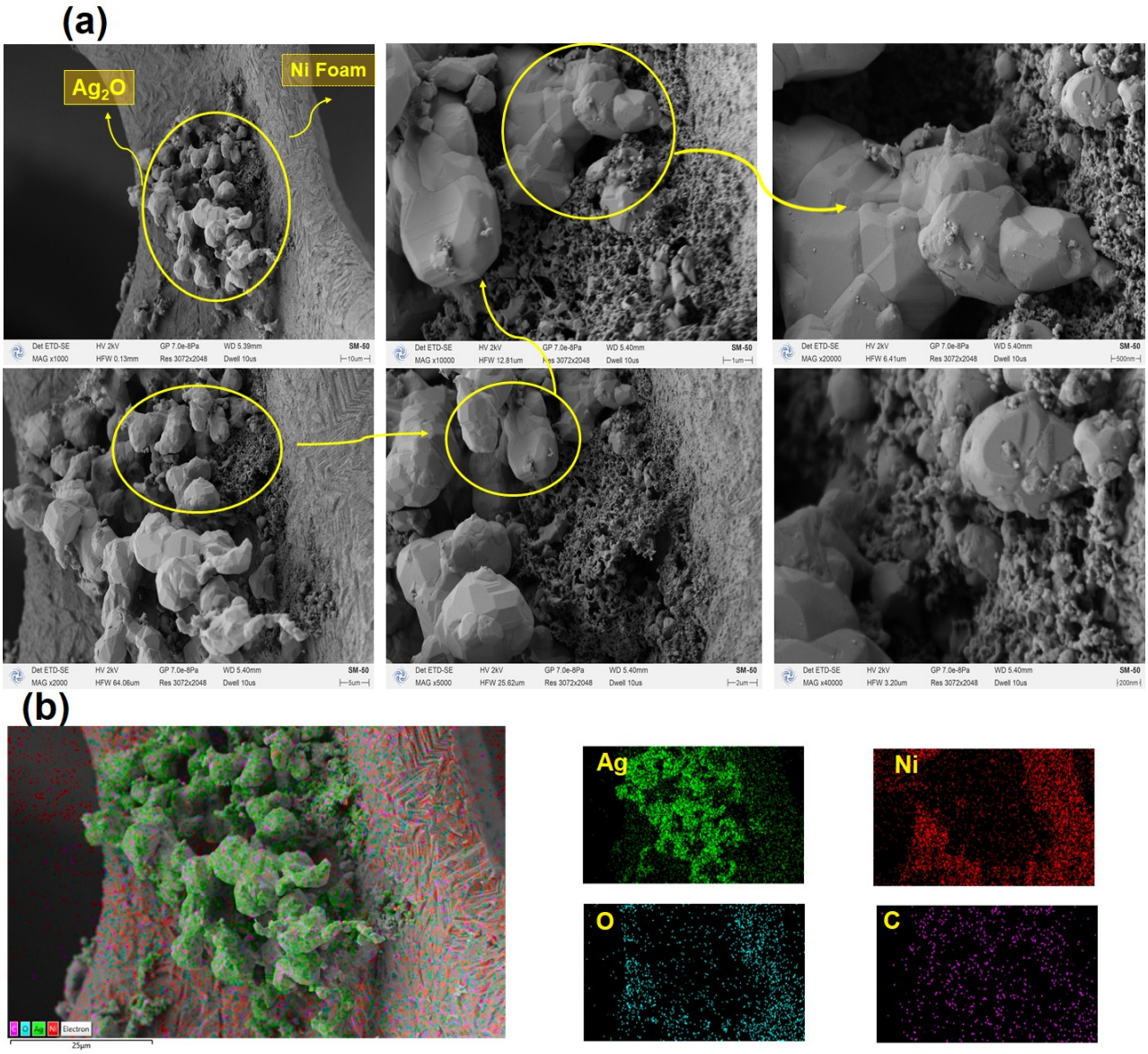

Fig. S25: FESEM (a), and elemental mapping (b) images of Ag_2O nanostructures hydrothermally synthesized on nickel foam (Ag_2O consists of small cubic or hexagonal particles that assemble into smooth surface).

Table S1: PXRD data for all nanocompounds.

Compounds	Mn_2O_3 peaks	Ag_2O peaks
Mn_2O_3	23.16° (211), 33.12° (222), 38.56° (400), 45.50° (332), 49.72° (431), 54.30° (521), 55.46° (440), 61.11° (611), 64.28° (541), 66.02° (622), 67.64° (631)	-
AM-1	23.83° (211), 33.17° (222), 38.76° (400), 55.32° (440), 66.10° (622), 67.89° (631)	27.98° (110), 32.46° (111), 46.40° (211), 57.67° (221), 76.60° (123)
AM-2	23.40° (211), 33.10° (222), 38.71° (400), 55.65° (440), 66.23° (622), 67.89° (631)	27.96° (110), 32.32° (111), 46.41° (211), 57.98° (221), 76.37° (123)
AM-3	23.66° (211), 33.20° (222), 38.69° (400), 55.65° (440), 66.35° (622), 67.99° (631)	28.23° (110), 32.32° (111), 46.42° (211), 57.72° (221), 76.18° (123)
AM-4	23.52° (211), 33.38° (222), 38.87° (400), 55.41° (440), 66.40° (622), 67.94° (631)	28.27° (110), 32.29° (111), 46.54° (211), 57.94° (221), 77.24° (123)
AM-1@PANI(1:1)	33.26° (222), 55.06° (440), 67.66° (631)	28.02° (110), 32.46° (111), 46.32° (211), 57.72° (221), 76.96° (123)
AM-1@PANI(2:1)	33.66° (222), 54.96° (440), 67.62° (631)	27.90° (110), 32.32° (111), 46.28° (211), 57.60° (221), 77.04° (123)
AM-1@PANI(3:1)	33.40° (222), 55.70° (440), 67.96° (631)	28.04° (110), 32.48° (111), 46.44° (211), 57.88° (221), 76.92° (123)
AM-1@PANI(5:1)	33.08° (222), 54.88° (440), 67.56° (631)	27.92° (110), 32.36° (111), 46.36° (211), 58.04° (221), 77.12° (123)

Table S2: OER important data for all prepared materials.

Electrocatalyst	η (mV)@10,50, and 100 mA cm^{-2} for OER	TS (mV dec^{-1})	R_{ct} (Ω)	C_{dl} (mF cm^{-2})
Ag_2O/NF	424, -, -	230.2	-	1.71
Mn_2O_3/NF	363, 517, -	180.3	-	1.19
AM-1/NF	360, 437, 499	95.9	17.44	3.80
AM-2/NF	364, 459, 542	116.1	-	3.27
AM-3/NF	362, 448, 521	105.2	-	3.50
AM-4/NF	370, 485, 595	134.8	-	2.90
PANI/NF	404, 576, -	180	44.86	2.24
AM-1@PANI(1:1/NF)	333, 399,457	82.3	27.42	6.51
AM-1@PANI(2:1)/NF	319, 383, 437	80.9	26.03	9.07
AM-1@PANI(3:1/NF)	316, 375, 425	73.3	15.97	10.15
AM-1@PANI(5:1)/NF	309, 364, 410	68.9	6.65	12.18

η= Overpotential TS= Tafel slope R_{ct}= Charge transfer resistance C_{dl}= Double layer capacitance

Table S3: HER important data for all prepared materials.

Electrocatalyst	η (mV)@10,50, and 100 mA cm^{-2} for HER	TS (mV dec^{-1})	R_{ct} (Ω)
Ag_2O/NF	252, 425, -	239.7	-
Mn_2O_3/NF	279.5, 445, -	241.4	-
AM-1/NF	206, 316, 378	161.2	240.67
AM-2/NF	208, 328, 401	179.4	-
AM-3/NF	207, 320, 391	174.9	-
AM-4/NF	220, 335, 418	183	-
PANI/NF	233, 355, -	182.3	242.64
AM-1@PANI(1:1)/NF	191, 298, 350	153.4	180.09
AM-1@PANI(2:1)/NF	169, 263, 329	134.9	122.69
AM-1@PANI(3:1)/NF	158, 247, 308	128	111.82
AM-1@PANI(5:1)/NF	139, 230, 285	125.3	92.22

η= Overpotential TS= Tafel slope R_{ct}= Charge transfer resistance

Tabe S4: Cell voltage value for all prepared materials in self-supported two-electrode system

Electrocatalyst	**Cell voltage (V)@10 mA cm^{-2}**
NF‖NF	-
Ag_2O/NF‖Ag_2O/NF	-
Mn_2O_3/NF‖Mn_2O_3/NF	1.970
AM-1/NF‖AM-1/NF	1.823
AM-2/NF‖AM-2/NF	1.90
AM-3/NF‖AM-3/NF	1.887
AM-4/NF‖AM-4/NF	1.940
AM-1@PANI(1:1)/NF‖AM-1@PANI(1:1)/NF	1.757
AM-1@PANI(2:1)/NF‖AM-1@PANI(2:1)/NF	1.728
AM-1@PANI(3:1)/NF‖AM-1@PANI(3:1)/NF	1.726
AM-1@PANI(5:1)/NF‖AM-1@PANI(5:1)/NF	1.620

AM=Ag_2O/Mn_2O_3